BNL-222748-2022-TECH

EIC-ADD-TN-026

EIC Transverse emittance growth due to crab cavity RF noise: Estimates and mitigation

K. Smith

February 2022

Electron-Ion Collider

Brookhaven National Laboratory

U.S. Department of Energy

USDOE Office of Science (SC), Nuclear Physics (NP) (SC-26)

DISCLAIMER

EIC TECHNICAL NOTE	NUMBER **EIC-ADD-TN-026**
AUTHORS: K. Smith (BNL), T. Mastoridis, P. Fuller, P. Mahvi, Y. Matsumura (California Polytechnic State University)	DATE 02/09/2022
EIC Transverse Emittance Growth due to Crab Cavity RF Noise: Estimates and Mitigation	

Abstract

The Electron-Ion Collider (EIC) requires crab cavities to compensate for a 25 mrad crossing angle and achieve maximum luminosity. The crab cavity Radio Frequency (RF) system will inject low levels of noise to the crabbing field, generating transverse emittance growth and potentially limiting luminosity lifetime. In this work, we estimate the transverse emittance growth rate as a function of the Crab Cavity RF noise and quantify RF noise specifications for reasonable performance. Finally, we evaluate the possible mitigation of the RF noise induced emittance growth via a dedicated feedback system.

1. Introduction

A theoretical formalism evaluating the transverse emittance growth rate due to RF phase ($\sigma_{\Delta\phi}$) and amplitude ($\sigma_{\Delta A}$, $\Delta A = \Delta V/V$) noise was derived in [1] and is shown in Equations 1 and 2 respectively:

$$\begin{aligned}
\left(\frac{d\epsilon_{x,y}}{dt}\right)_{\Delta\phi} &= N_{cavities}\beta_{cc}\left(\frac{eV_o f_{rev}}{2E_b}\right)^2 \left\{e^{-\sigma_\phi{}^2}\left[I_o\left[\sigma_\phi{}^2\right] + 2\sum_{l=1}^{\infty} I_{2l}\left[\sigma_\phi{}^2\right]\right]\right\} \sum_{k=-\infty}^{\infty}\int_{-\infty}^{\infty} S_{\Delta\phi}\left[(k \pm \nu_b) f_{rev}\right]\rho\left(\nu_b\right) d\nu_b \\
&= N_{cavities}\beta_{cc}\left(\frac{eV_o f_{rev}}{2E_b}\right)^2 C_{\Delta\phi}(\sigma_\phi)\,\frac{2\sigma_{\Delta\phi}^2}{f_{rev}} \\
&= \frac{1}{N_{cavities}\beta^*}\left[\left(\frac{ec\theta_{cc} f_{rev}}{4\omega_{RF}}\right)^2\right] C_{\Delta\phi}(\sigma_\phi)\,\frac{2\sigma_{\Delta\phi}^2}{f_{rev}}
\end{aligned} \tag{1}$$

$$\begin{aligned}
\left(\frac{d\epsilon_{x,y}}{dt}\right)_{\Delta A} &= N_{cavities}\beta_{cc}\left(\frac{eV_o f_{rev}}{2E_b}\right)^2 \left\{e^{-\sigma_\phi{}^2}\sum_{l=0}^{\infty} I_{2l+1}\left[\sigma_\phi{}^2\right]\right\} \sum_{k=-\infty}^{\infty}\int_{-\infty}^{\infty} S_{\Delta A}\left[(k \pm \nu_b \pm \nu_s) f_{rev}\right]\rho\left(\nu_b\right) d\nu_b \\
&= \frac{1}{N_{cavities}\beta^*}\left[\left(\frac{ec\theta_{cc} f_{rev}}{4\omega_{RF}}\right)^2\right] C_{\Delta A}(\sigma_\phi)\,\frac{4\sigma_{\Delta A}^2}{f_{rev}}
\end{aligned} \tag{2}$$

Here, $\epsilon_{x,y}$ is the transverse emittance (horizontal or vertical depending on the crabbing plane, horizontal for the EIC), $N_{cavities}$ is the number of crab cavities, β_{CC} is the beta function at the crab cavity location, e is the charge of a proton, V_o is the effective transverse deflecting voltage of the crab cavity, f_{rev} is the revolution frequency, E_b the beam energy, σ_ϕ the rms bunch length (in radians with respect to the RF frequency), I the modified Bessel function of the first kind, ν_b the mean betatron tune, ν_s the mean synchrotron tune, $\beta^*$the beta function at the interaction point, θ_{cc} the crabbing angle, $S_{\Delta\phi}$, $S_{\Delta A}$ the phase and relative amplitude noise power spectral density respectively (with units of rad^2/Hz and 1/Hz respectively), and $\rho(\nu_b)$ the tune distribution. The voltage power spectral density is $S_{\Delta V} = V^2 S_{\Delta A}$. The $\pm$ sign refers to upper and lower sidebands. The total phase and amplitude noise power sampled by the beam are $\sigma_{\Delta\phi}^2$ and $\sigma_{\Delta A}^2$ respectively. As the crab cavity RF zero phase is set at the center of the bunch, phase noise kicks lead to a shift of the bunch's centroid position, whereas amplitude noise leads to a rotation of the bunch around its centroid.

There are three components in these equations:

- The operational and accelerator parameters are shown in blue. There is little or no control of these values. This term is effectively inversely proportional to $1/\beta^*$ for a given full crabbing angle θ_{cc}.
- The bunch length dependence is shown in red. This term is almost constant over the EIC operational range.
- The RF noise power spectral density sampled by the beam is shown in black. This term depends on the RF and LLRF technology, and cannot be evaluated at this time, since these systems are under design.

2. Simulation Results

Simulations were performed to confirm the above relationships for the EIC, using PyHEADTAIL, a macro-particle tracking code that simulates collective beam dynamics [2].

2.1 Emittance Growth Rate with Noise Power

We first investigated the emittance growth rate dependence on noise power. There is a linear relationship between emittance growth rate and noise power, as expected from the theoretical expressions, for both phase and amplitude noise. Figures 1 and 2 show the results for the Electron Storage Ring (ESR). Simulations of the Hadron Storage Ring (HSR) produced similar results.

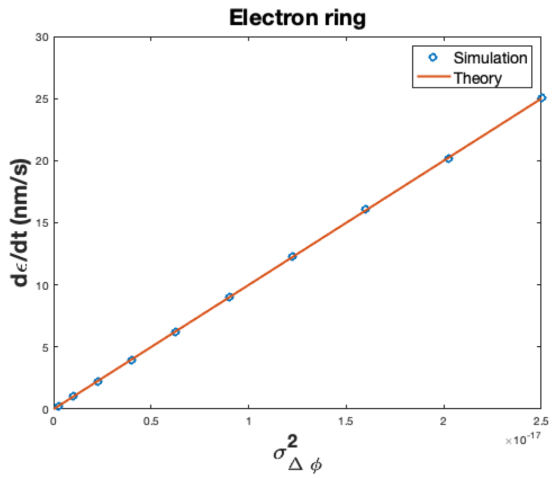

Figure 1: Emittance growth rate with phase noise power (ESR).

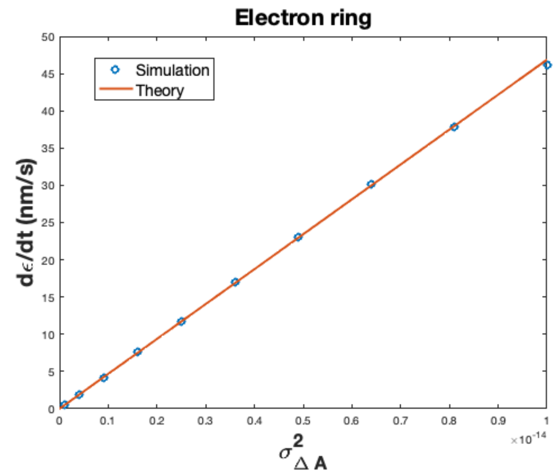

Figure 2: Emittance growth rate with amplitude noise power (ESR).

2.2 Emittance Growth Rate with Bunch Length

We then checked the emittance growth rate dependence on bunch length. The EIC bunch length is low enough for both rings so that the bunch length coefficient is almost 1 for phase noise and close to 0 for amplitude noise. Simulations were performed in a narrow range around the planned bunch length. Once again, there was very good agreement between simulations and the theoretical expressions, as shown in Figures 3 and 4.

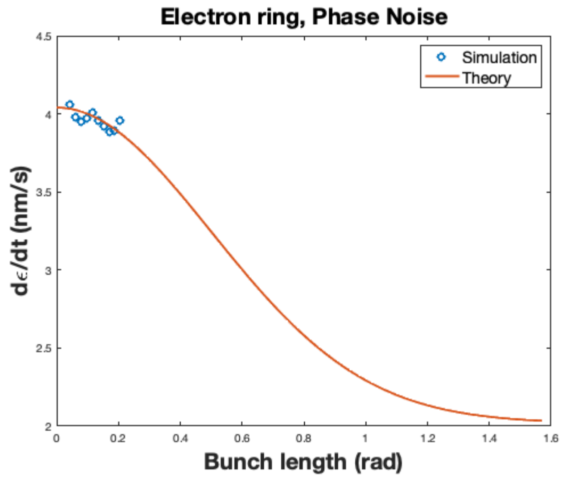

Figure 3: Emittance growth rate with bunch length (phase noise, ESR).

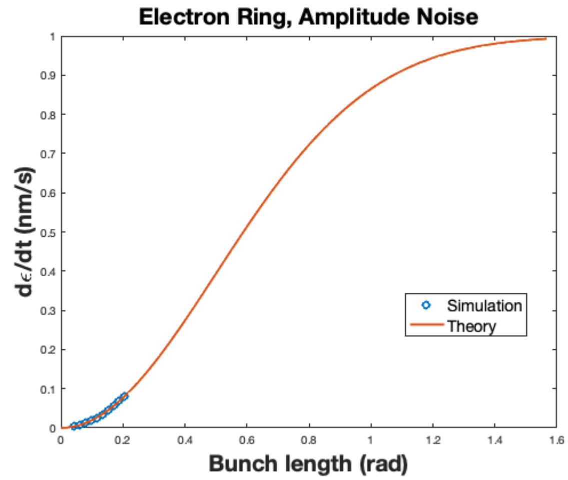

Figure 4: Emittance growth rate with bunch length (amplitude noise, ESR).

3. Bunch Length Effect on Transverse Emittance Growth

EIC ESR and HSR bunch lengths vary depending on the collision energy and hadron species. The verified theoretical expressions were used to estimate the effect of the planned EIC bunch lengths on the EIC transverse emittance growth rates due to RF noise. The results were also compared to the High-Luminosity Large Hadron Collider (HL-LHC).

The term $C_{\Delta\phi}(\sigma_\phi)$ in Equation 3 shows the scaling of the phase noise effect due to the bunch length. Similarly, the term $C_{\Delta A}(\sigma_\phi)$ in Equation 4 shows the scaling of the amplitude noise effect. σ_φ is the bunch length in radians with respect to the crab cavity frequency.

$$C_{\Delta\phi}(\sigma_\phi) = \left\{ e^{-\sigma_\phi{}^2} \left[I_o\left[\sigma_\phi{}^2\right] + 2\sum_{l=1}^{\infty} I_{2l}\left[\sigma_\phi{}^2\right] \right] \right\} \tag{3}$$

$$C_{\Delta A}(\sigma_\phi) = \left\{ e^{-\sigma_\phi{}^2} \sum_{l=0}^{\infty} I_{2l+1}\left[\sigma_\phi{}^2\right] \right\} \tag{4}$$

Table 1 shows the relevant parameters for the ESR and HSR collision energies, and for the HL-LHC for comparison, as well as the resulting estimate for $C_{\Delta\phi}(\sigma_\phi)$ and $C_{\Delta A}(\sigma_\phi)$.

	σ_z (cm)	**σ_φ (rad)**	**$C_{\Delta\varphi}$**	**$C_{\Delta A}$**
HL-LHC	7.5	0.630	0.726	0.137
ESR 5 GeV	0.7	0.058	0.996	0.002
ESR 10 GeV	0.7	0.058	0.996	0.002
ESR 18 GeV	0.9	0.074	0.995	0.003
HSR 41 GeV	7.5	0.309	0.913	0.043
HSR 100 GeV	7	0.289	0.922	0.038
HSR 275 GeV	6	0.248	0.942	0.029
Au 41 GeV	11.6	0.479	0.816	0.092
Au 110 GeV	7	0.289	0.922	0.038

Table 1: HL-LHC and EIC ESR/HSR bunch length and $C_{\Delta\phi}(\sigma_\phi)$, $C_{\Delta A}(\sigma_\phi)$ terms.

Clearly, there is lower sensitivity to amplitude noise in the EIC than in the HL-LHC due to the shorter bunch length, especially for the ESR. This is significant if a bunch-by-bunch transverse feedback system is employed in the EIC. Such a system acts on the bunch centroid and can thus only counteract the effects of phase noise in the crabbing system. Since phase noise is dominant in the EIC, a bunch-by-bunch transverse feedback can *considerably* reduce transverse emittance growth due to crab cavity RF noise.

4. RF Noise Requirements

Using Equations 1 and 2, we can then set an RF noise requirement to achieve a target transverse emittance growth rate.

4.1 Parameters

Table 2 shows the operational parameters used for each ring and energy level. Of particular interest is the full crabbing angle θ_{CC}, since the sensitivity to noise scales as θ_{CC}^2.

	Energy (GeV)	**θ_{CC} (mrad)**	**β^* (m)**	**$N_{cavities}$**	**f_{rev} (Hz)**	**f_{RF} (MHz)**
HL-LHC	7000	0.38	0.15	4	11245	400.8
ESR 5 GeV	5	25	1.15	2	78195	394
ESR 10 GeV	10	25	1.31	2	78195	394
ESR 18 GeV	18	25	0.76	2	78195	394
HSR 41 GeV	41	25	1.18	8	78195	197
HSR 100 GeV	100	25	0.9	8	78195	197
HSR 275 GeV	275	25	0.9	8	78195	197
Au 41 GeV	41	25	1.18	8	78195	197
Au 110 GeV	110	25	0.9	8	78195	197

Table 2: HL-LHC and EIC ESR/HSR operational parameters.

4.2 Target Transverse emittance growth rate

The target emittance growth rate for the HL-LHC is 1%/hr to minimize the impact on luminosity. For the EIC ESR, the emittance growth rate must be lower than the emittance damping time due to synchrotron radiation. For the HSR, the emittance growth rate target is set equal to the IBS growth rate. This is possibly an optimistic threshold since the EIC Strong Hadron Cooling is designed to just counteract the IBS to maintain luminosity. There are also additional sources of growth (beam-beam effects for example). So, the HSR thresholds might have to be further adjusted lower. The relevant parameters are summarized in Table 3, where τ_{IBS} is the IBS growth time and τ_d the transverse radiation damping time.

	ε_x (nm)	**τ_{IBS} (hr)**	**τ_d (ms)**	**$d\varepsilon/dt_{target}$ (nm/hr)**	**$d\varepsilon/dt_{target}$ (%/hr)**
HL-LHC	0.335			0.00335	1
ESR 5 GeV	20		73	362840	1814200
ESR 10 GeV	20		73	362840	1814200
ESR 18 GeV	24		125	254278	1059493
HSR 41 GeV	44	3.4		4.76	10.8
HSR 100 GeV	26	2		4.78	18.4
HSR 275 GeV	11.3	2		2.08	18.4
Au 41 GeV	68	0.16		156	230

Au 110 GeV	42	0.89		17.4	41.3

Table 3: HL-LHC and EIC ESR/HSR target emittance growth rates.

As expected, the ESR target growth rate is many orders of magnitude higher than the rate for the HSR due to the strong synchrotron radiation damping. The HSR also has much higher target rates than the HL-LHC. This is due to the very tight HL-LHC specification to achieve minimal impact on luminosity and the much lower transverse emittance.

4.3 Sampled noise threshold

Table 4 summarizes the RF noise thresholds for phase and amplitude noise calculated using Equations 1 and 2, for the HL-LHC, and the EIC ESR and HSR.

	$\sigma_{\Delta\varphi}$ (μrad)	**$\sigma_{\Delta A}$ (1e-6)**
HL-LHC	8.17	13.30
ESR 5 GeV	805	12700
ESR 10 GeV	860	13600
ESR 18 GeV	548	7060
HSR 41 GeV	3.09	10.1
HSR 100 GeV	2.69	9.36
HSR 275 GeV	**1.75**	**7.07**
Au 41 GeV	18.7	39.4
Au 110 GeV	5.12	17.8

Table 4: HL-LHC and EIC ESR/HSR crab cavity RF noise thresholds.

The much higher EIC crabbing angle leads to a significantly higher sensitivity to noise compared to the HL-LHC, as shown in Equation 3 and Table 1. Since the transverse emittance growth rate scales as θ_{CC}^2, the EIC sensitivity to RF noise power is 4000 times higher than the HL-LHC. On the other hand, the emittance growth rate target for the HL-LHC is three orders of magnitude lower than for the EIC HSR, and eight orders of magnitude lower than the EIC ESR. Most other parameters are comparable, and as a result, the EIC HSR noise thresholds are in the same order of magnitude, but still lower than the already challenging levels required for the HL-LHC. The EIC ESR thresholds are much higher due to the fast transverse radiation damping time.

5. 394 MHz cavities in the HSR

The Full Scope EIC plan includes 394 MHz cavities in the HSR to improve the crab kick linearity. Table 5 summarizes the parameters in this scheme.

Energy (GeV)	$N_{cavities}$	β_{CC} (m)	f_{RF} (MHz)	$C_{\Delta\varphi}$	$C_{\Delta A}$	$\sigma_{\Delta\varphi}$ (μrad)	$\sigma_{\Delta A}$ (1e-6)
41	8	200	197	0.913	0.043	1.91	5.96
	4	200	394	0.732	0.134		
100	8	500	197	0.922	0.038	1.90	6.35
	4	500	394	0.756	0.122		
275	8	1300	197	0.942	0.029	1.24	4.78
	4	1300	394	0.806	0.097		

Table 5: EIC HSR Full Scope parameters with 197 MHz crab cavities.

The noise requirement is lowered by a factor of about 1.5. The 394 MHz do not actually contribute much to the noise sampled by the beam. Rather, it is the increase of the 197 MHz cavity voltage that increases the noise power.

6. RF Noise Spectrum and Sampled Noise

For the purposes of the Low-Level RF (LLRF) design, these noise levels should be converted to a power spectral density. The total noise power sampled by the beam is related to the power spectral density by:

$$2\sigma_\phi^2 = \sum_{k=-\infty}^{\infty} \int_{-\infty}^{\infty} S_{\Delta\phi}\left[(k \pm \nu_b) f_{rev}\right] \rho\left(\nu_b\right) d\nu_b f_{rev} \tag{5}$$

The higher EIC revolution frequency reduces the beam sampled power, since there are fewer revolution harmonics within the closed loop bandwidth of the crab cavity response.

Figure 5 shows the LHC accelerating cavities noise power spectral density $S_{\Delta\phi}(f)$ for reference, and the HL-LHC and EIC crab cavity RF noise estimates, as well as the corresponding beam sampling. The LHC Main RF PSD includes $1/f^2$ noise up to ~10 Hz, RF reference noise up to ~1 kHz, transmitter noise to ~20 kHz, and then a noise plateau at ~-133 dBc/Hz due to the demodulation of the cavity antenna signal.

The HL-LHC estimate assumes improved RF reference noise (below the demodulation level). It also assumes IOTs or Tetrodes instead of klystrons, so that the transmitter noise is also below the demodulation level. The LLRF design will be improved to bring the noise due to the demodulation down to -143 dBc/Hz. Finally, the closed loop bandwidth of the RF loop will be reduced significantly to ~50 kHz[1].

[1] A possible tradeoff of this narrowband design with transverse instability control will be studied.

The EIC estimate similarly includes a relatively low closed loop bandwidth of ~50 kHz. The LLRF noise plateau is set to -151 dBc/Hz, which is possibly the lowest level achieved in an actual or proposed accelerator design [3]. This is possibly an optimistic and challenging design choice.

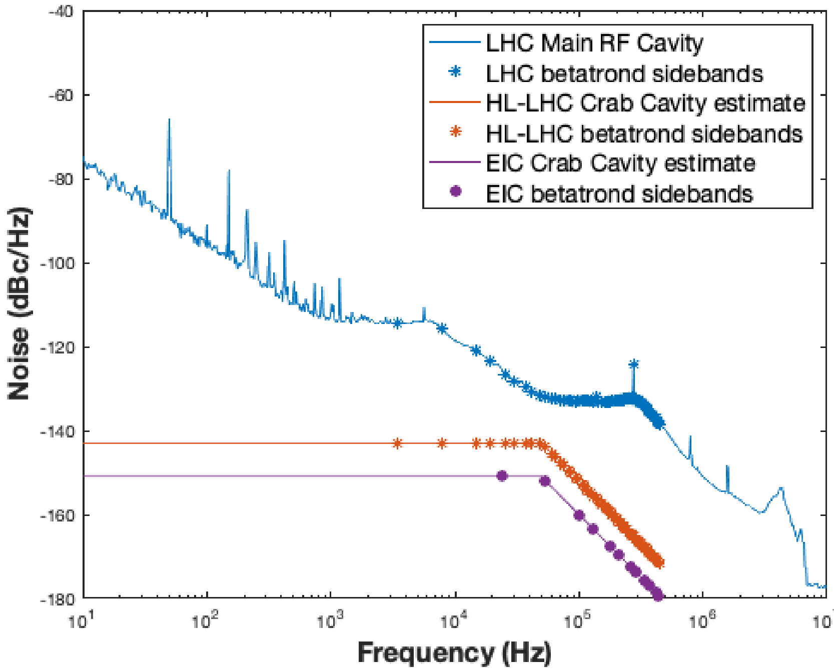

Figure 5: RF noise power spectral density $S_{\Delta\phi}(f)$ for LHC accelerating cavities and HL-LHC/EIC crab cavity estimate.

As seen in Figure 5, the EIC beam would sample 6.5 times lower noise power than the HL-LHC beam for the same spectrum. For a given $\sigma_{\Delta\varphi}$ and $\sigma_{\Delta A}$ level though, the threshold power spectral density is largely unchanged due to the f_{rev} scaling between the emittance growth rate and the sampled noise power, as seen in Equations 1 and 2.

The resulting rms sampled noise is $\sigma_{\phi} = 27$ µrad for the HL-LHC and 11 µrad for the EIC. So, even with this extremely low RF noise PSD, the rms sampled noise is an order of magnitude higher than the target.

6.1 LLRF Design

It is evident from Figure 5 that the LLRF design will significantly impact the RF noise spectrum. Therefore, the crab cavity LLRF design should be carefully studied, especially given the added complexity of regulating the individual station voltages, while ensuring that the total crabbing/uncrabbing voltage is zero.

There are potential architectures that could reduce the noise sampled by the beam. For example, an architecture should be evaluated where the LLRF on the vectorial sum is wideband, but each individual station has a very slow regulation far below the first betatron sideband. High frequency perturbations would be present in the individual stations but would be considerably reduced on the cavity sum. Since the total noise power sampled by the beam is the sum of the noise power injected by each section, this architecture would lead to a *significant* reduction in the noise power sampled by the beam in the HSR, given the high number of cavities per IP. This architecture assumes that crab cavity impedance reduction in the HSR is not critical. This assumption should be carefully evaluated.

7. Crab Cavity RF Noise Feedback

The RF noise sensitivity is therefore very high in the EIC. The RF noise threshold for the HSR is significantly lower than the technological state of the art. Therefore, a mitigation of the crab cavity RF noise effects is required.

A dedicated feedback system could mitigate these effects. A similar system is planned for the HL-LHC [4], [5]. A simplified block diagram of this system is shown in Figure 6.

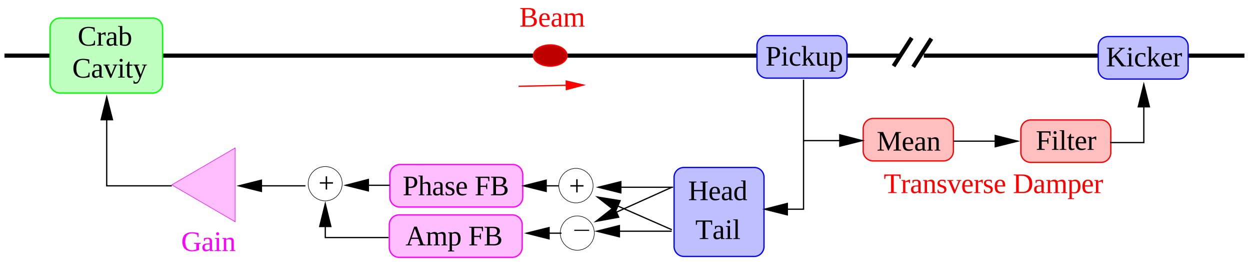

Figure 6: Block diagram for proposed crab cavity RF noise feedback system.

The bunch head and tail position would be extracted from the pickup signal. Since we are concerned with the residual noise after *all* the crabbing and uncrabbing cavities, the pickup should be outside the IR region. The head/tail difference and sum estimate the bunch tilt and offset (due to amplitude and phase noise respectively).

We conducted simulations of such a system for the EIC HSR to study its potential performance and limitations. We used the following parameters: tune spread of 3e-3, β_{CC} = 500 m, E_b = 100 GeV, and V_{CC} = 3.57 MV.

7.1 Emittance Growth with Feedback Gain

As shown in Figures 7 and 8, an *ideal* Crab Cavity Noise Feedback system has the potential to significantly reduce both the phase (left) and amplitude (right) noise effects on transverse emittance growth.

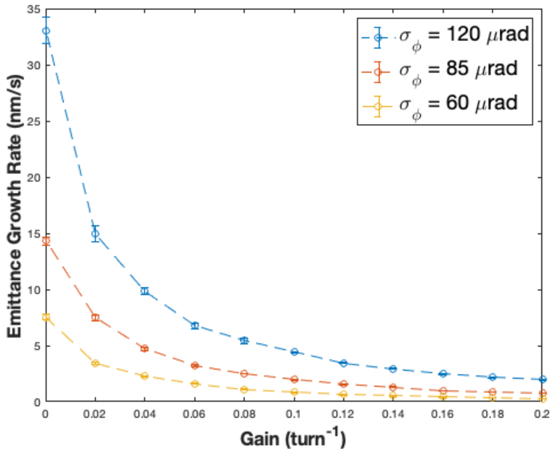

Figure 7: Emittance growth rate with feedback gain (phase noise).

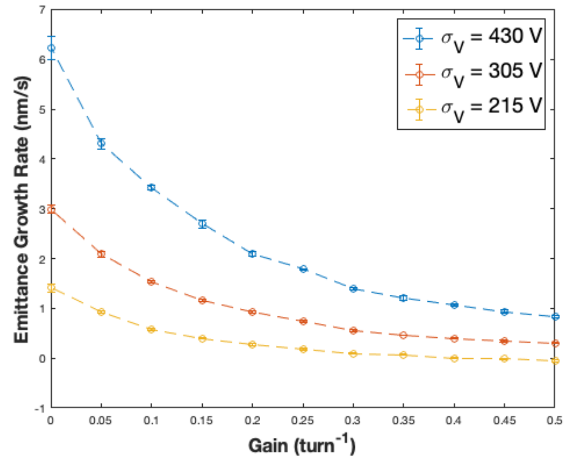

Figure 8: Emittance growth rate with feedback gain (amplitude noise).

It should be noted that even though the emittance growth rates might appear unreasonably high, the *total* emittance growth over the course of the simulation is comparable to an EIC coast.

We then incorporated non-idealities in the simulation, that would limit the system's performance.

7.2 Emittance Growth with Tune Spread

The feedback system can mitigate the noise effects if the feedback damping time is shorter than the decoherence time. As the tune spread is increased, the system's effectiveness is reduced (for a fixed system delay), as shown in Figure 9. The range of tune spread values is probably conservative on the high end, but the conclusion is still valid: any changes of the operational tune spread value will negatively impact the performance of the crab cavity noise feedback system.

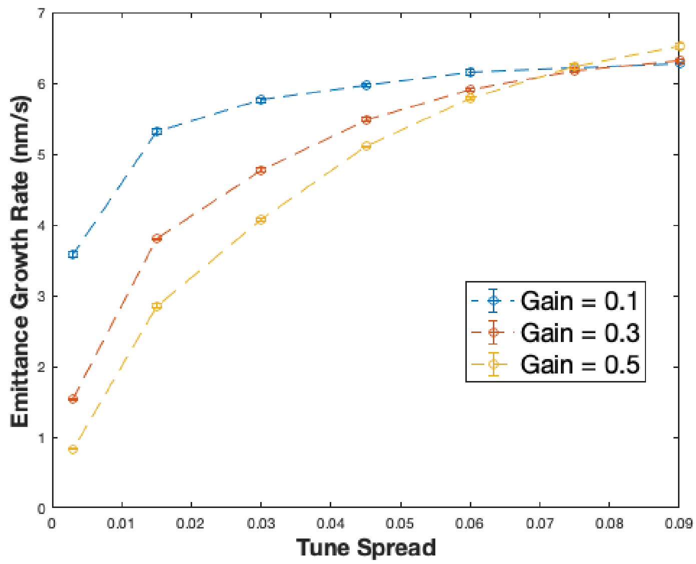

Figure 9: Emittance growth rate with tune spread.

7.3 Emittance Growth with Delay

For similar reasons, an increase of the system's delay, leads to a performance reduction, as shown in Figure 10. In addition, high system delay leads to feedback loop instability for high gain settings. It is clear that the system is unstable when the delay exceeds 9 turns for a gain of 0.3 and when it exceeds 5 turns for a gain of 0.5.

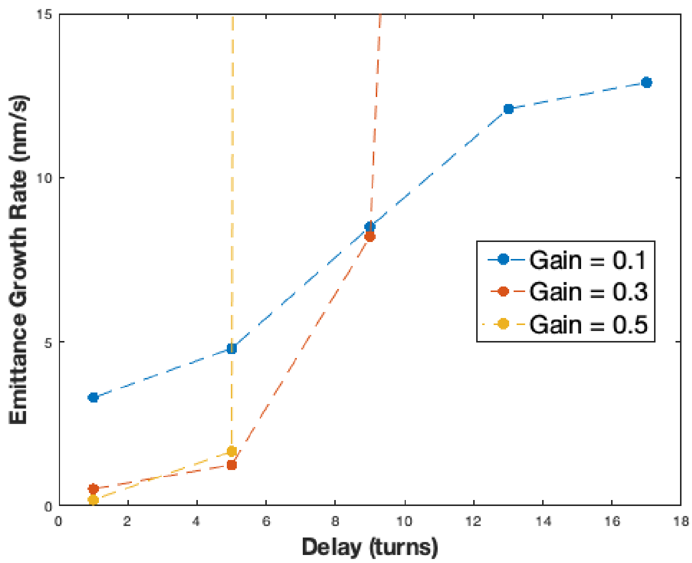

Figure 10: Emittance growth rate with system delay.

7.4 Measurement noise

The most important limitation to the system performance though is the pickup precision. Measurement noise was injected in the simulation to study this effect. As expected, the transverse emittance growth rate is dominated by the crab cavity RF noise for low feedback gains but is dominated by the measurement noise for high gains, as seen in Figure 11. Simplistically, when the gain is high, the feedback system can suppress the crab cavity RF noise, but it also amplifies the measurement noise to the point that it leads to significant emittance growth.

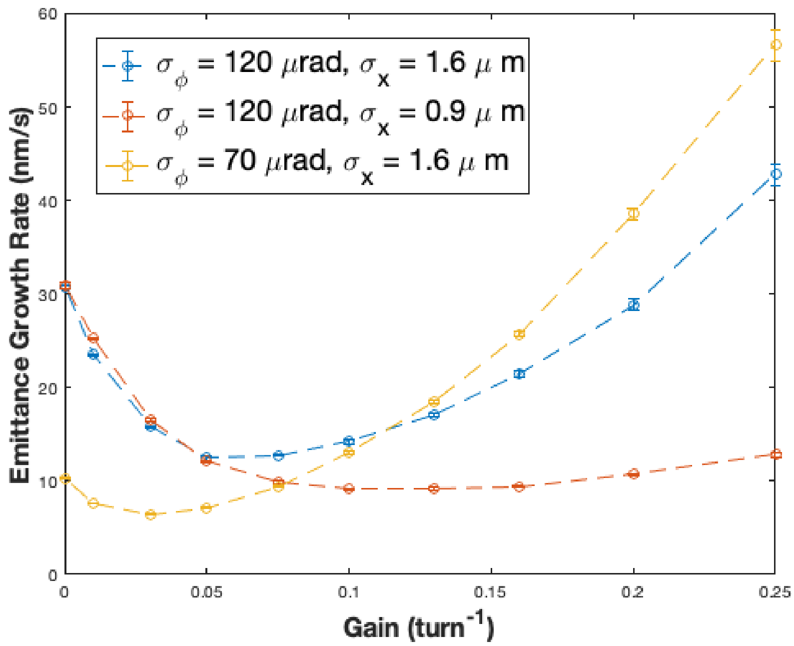

Figure 11: Emittance growth rate with feedback gain in the presence of measurement noise.

It should be noted that the sensitivity to measurement noise will *highly* depend on the crab cavity and pickup β function ratio. Ideally, the pickup would be placed at a high β location to minimize the effect of measurement noise. The pickup should also have a $\pi/2$ phase advance with respect to the crab cavity. Figure 12 shows the smaller dependence to measurement noise (σ_x), when the pickup is placed at a location with ten times higher β value.

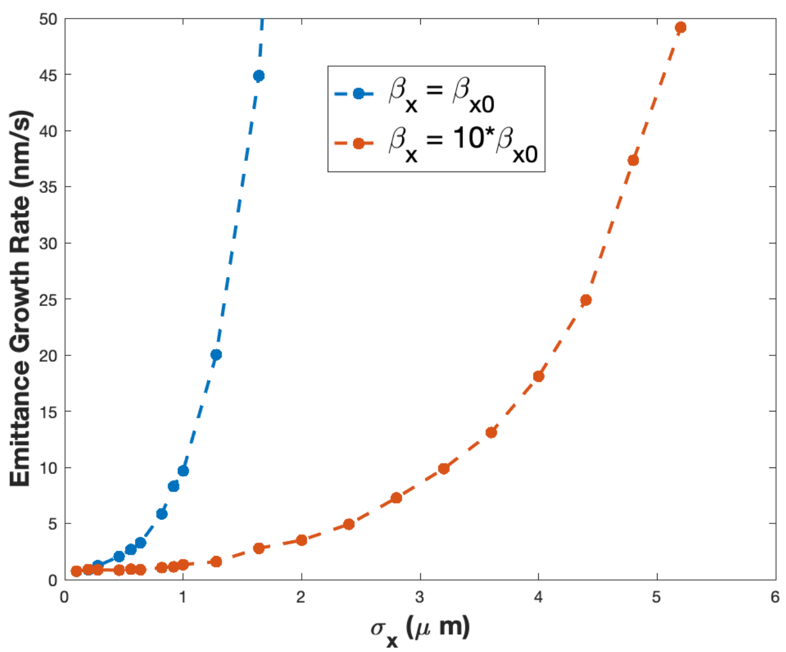

Figure 12: Emittance growth rate with phase noise power (ESR).

8. Conclusions and future steps

The sensitivity to RF noise is *very* high in the EIC. The RF noise threshold for the HSR will be very hard to achieve technologically. Thus, a mitigation of the crab cavity RF noise effects is required.

A dedicated feedback system could reduce the crab cavity RF noise effects and thus relax the crab cavity RF noise threshold. The performance of the system will *greatly* depend on the pickup precision, location, and additional technical specifications (signal processing/equalization, longitudinal motion effects, etc.). On the other hand, the precision requirements could be relaxed by averaging over many bunches, taking advantage of the low crab cavity closed-loop bandwidth. To a lesser extent, the crab cavity noise feedback system performance will also depend on the tune spread and the system delay.

The pickup is a *critical* component for this system and the immediate future steps should be focused on its specifications. An estimate of the pickup performance is necessary to determine precision specifications, which in turn will allow us to estimate the crab cavity RF noise threshold in the presence of the dedicated noise feedback system.

In parallel, the crab cavity LLRF design should be studied. The LLRF should regulate individual station voltages *and* the total crabbing/uncrabbing voltage, while keeping the noise injected to the beam as low as possible. Tradeoffs probably exist between low noise and high impedance control architectures. These tradeoffs should be carefully quantified.

It should be noted that the estimates and simulations presented here do *not* include coupling with the machine transverse impedance. HL-LHC simulations have shown a potential reduction of RF noise effects due to this coupling. This reduction is up to a factor of two for *phase* noise, but there is no reduction for *amplitude* noise [6].

References

[1] P. Baudrenghien, T. Mastoridis, *Transverse emittance growth due to RF noise in the high-luminosity LHC crab cavities*, Phys. Rev. ST Accel. Beams 18 (2015) 101001.

[2] A. Oeftiger, *An Overview of PyHEADTAIL*, CERN-ACC-NOTE-2019-0013, April 2019.

[3] G. Huang, L.R. Doolittle, J. Yang, Y. Xu, *Low Noise Digitizer Design for LCLS-II*, Proceedings of NAPAC2016, Chicago, IL, USA, October 2016.

[4] P. Baudrenghien, T. Mastoridis, *Crab Cavity RF Noise Feedback and Transverse Damper Interaction*, CERN-ACC-NOTE-2019-0006, March 2019.

[5] T. Mastoridis, P. Baudrenghien, *Transverse emittance growth due to RF Noise in Crab Cavities: Theory, Measurements, Cure, and High-Luminosity LHC estimates*, in preparation for publication.

[6] N. Triantafyllou, F. Antoniou, H. Bartosik, P. Baudrenghien, X. Buffat, R. Calaga, Y. Papaphilippou, T. Mastoridis, L.R. Carver, A. Wolski, *Investigation of Damping Effects of the Crab Cavity Noise Induced Emittance Growth*, prepared for publication in IPAC 2021 Proceedings.